

## SOLUTION OF $F(z+1) = \exp(F(z))$ IN COMPLEX $z$ -PLANE

DMITRII KOUZNETOSV

ABSTRACT. Tetration  $F$  as analytic solution of equations  $F(z-1) = \ln(F(z))$ ,  $F(0) = 1$  is considered. The representation is suggested through the integral equation for values of  $F$  at the imaginary axis. Numerical analysis of this equation is described. The numerical solution for  $F$  remains finite at the imaginary axis, approaching eigenvalues  $L, L^*$  of logarithm ( $L = \ln L$ ). Smallness of the residual indicates existence of unique tetration  $F(z)$ , that grows along the real axis and is limited along the imaginary axis, being analytic in the whole complex  $z$ -plane except singularities at integer  $z < -1$  and the cut at  $z < -2$ . Application of the same method for other cases of the Abel equation is discussed.

### 1. INTRODUCTION

The practical ability to deal with big numbers depends on their representation. The positional numeral system allowed to write the most of required numbers during centuries. Invention of the floating point enabled huge numbers, although the “floating overflow” still occurs, if the logarithm of a number happens to be too large. The range of huge numbers, distinguishable from infinity in computational mathematics, can be drastically extended, using a function with fast growth [1], for example, the Ackermann functions [2]. Perhaps, the fourth of the Ackermann functions provides the growth fast enough for the requests of this century. This function  $A(4, x)$  can be expressed in form

$$(1.1) \quad A(4, x) = \underbrace{2^{2^{\cdot^{\cdot^2}}}}_{x-3 \text{ times}} - 3 = \exp_2^{x-3}(1) - 3,$$

where

$$(1.2) \quad \exp_a^z(t) = \underbrace{\exp_a \left( \exp_a \left( \dots \exp_a(t) \dots \right) \right)}_{z \text{ exponentials}},$$

means application of the exponential  $z$  times. Various names are used for the this operation: “generalized exponential function” [1], “ultraexponentiation” [3], “Superexponentiation” [4], “tetration” [5]. I use the shortest one, “tetration”. This name indicates that this operation is forth in the hierarchy of operations, after summation, multiplication and exponentiation. For the first three operations, the analytic extension for the complex values of the argument is established; and these operations are recognized as elementary functions [6, 7]. Tetration is not yet considered

---

Received by the editor May 7, 2008.

2000 *Mathematics Subject Classification*. Primary 30A99; Secondary 33F99 .

as a special function; the extension for real and complex values is not yet established; iteration of a transcendental function of a complex variable is not trivial [8, 9].

The tetration (1.2) can be written as the recurrent equation

$$(1.3) \quad \exp_a^z(t) = \exp_a(\exp_a^{z-1}(t)) \quad ; \quad \exp_a^0(t) = t \quad ,$$

for integer  $z > -2$ . In this paper, I consider only the case  $t=1$  ,  $a=e=\exp(1)$  . In order not to write the main argument  $z$  as superscript, let  $F(z) = \exp_e^z(1)$ ; then, for  $F$  I have the equation

$$(1.4) \quad F(z+1) = \exp(F(z)) \quad ,$$

mentioned in the title. Together with condition

$$(1.5) \quad F(0) = 1 \quad ,$$

equation (1.4) can be considered as definition of tetration of an integer argument, larger than  $-2$ ; it is special case of equation (1.2) at  $a = e$  and  $t = 1$ . Such a tetration, as well as the Ackermann functions [2] could be used as rapidly growing function to represent huge numbers in computers.

Equation (1.4), even together with condition (1.5), does not define an unambiguous function; additional requirements, assumptions are necessary to specify it. Such an assumption could be that  $F'(z)$  is continuous non-decreasing function in the range  $z > -1$ . This leads [3] to the piecewise uxp, which can be defined in the following way:

$$(1.6) \quad \text{uxp}(x) = \begin{cases} \log(\text{uxp}(z+1)) & \text{at} & \Re(z) \leq -1 \\ z+1 & \text{at} & -1 < \Re(z) \leq 0 \\ \exp(\text{uxp}(z-1)) & \text{at} & 0 < \Re(z) \end{cases}$$

This function is shown in the top of the figure 1(a); lines of constant amplitude and constant phase are drawn. Discontinuities (cuts) are marked with wide lines. At the real axis, function uxp has continuous derivative; it is analytic in the complex  $z$  plane with cuts at  $z \leq -2$  and at  $\Re(z) \in \text{integers}$ . These cuts separate the complex plane to almost independent segments. The figure arises questions, weather all these cuts are necessary, or some solutions of equation (1.4) are more regular. As a sketch of such a solution, in the figure 1b, I plot also the function

$$(1.7) \quad \text{Fit}_3(z) = \begin{cases} \log(\text{Fit}_3(z+1)) & \text{at} & \Re(z) \leq -1 \\ \text{fit}_3(z) & \text{at} & -1 < \Re(z) \leq 0 \\ \exp(\text{Fit}_3(z-1)) & \text{at} & 0 < \Re(z) \end{cases} ,$$

where

$$(1.8) \quad \text{fit}_3(z) = 0.6 \text{fit}_2(z) + 0.4 \ln(\text{fit}_2(x+1)) \quad ,$$

$$(1.9) \quad \text{fit}_2(z) = \ln(2+z) + (1+z) \left( 1 + \frac{z}{2} \exp((z-1)s_2(z)) \left( e^{-2+\ln \frac{4}{3}} - \ln 2 \right) \right) .$$

$$(1.10) \quad s_2(z) = \exp(\exp(z-2.51)) - 0.6 + 0.08(z+1) \quad ,$$

Function  $\text{Fit}_3$  has the same cuts of the range of analyticity, as function uxp, but in the range of figures 1(a,b), these jumps are small and are not seen.

In the following, I *assume* that there exist unique analytic tetration  $F$ , and it has properties, similar to those of the function  $\text{Fit}_3$  seen in figure 1b; then I guess

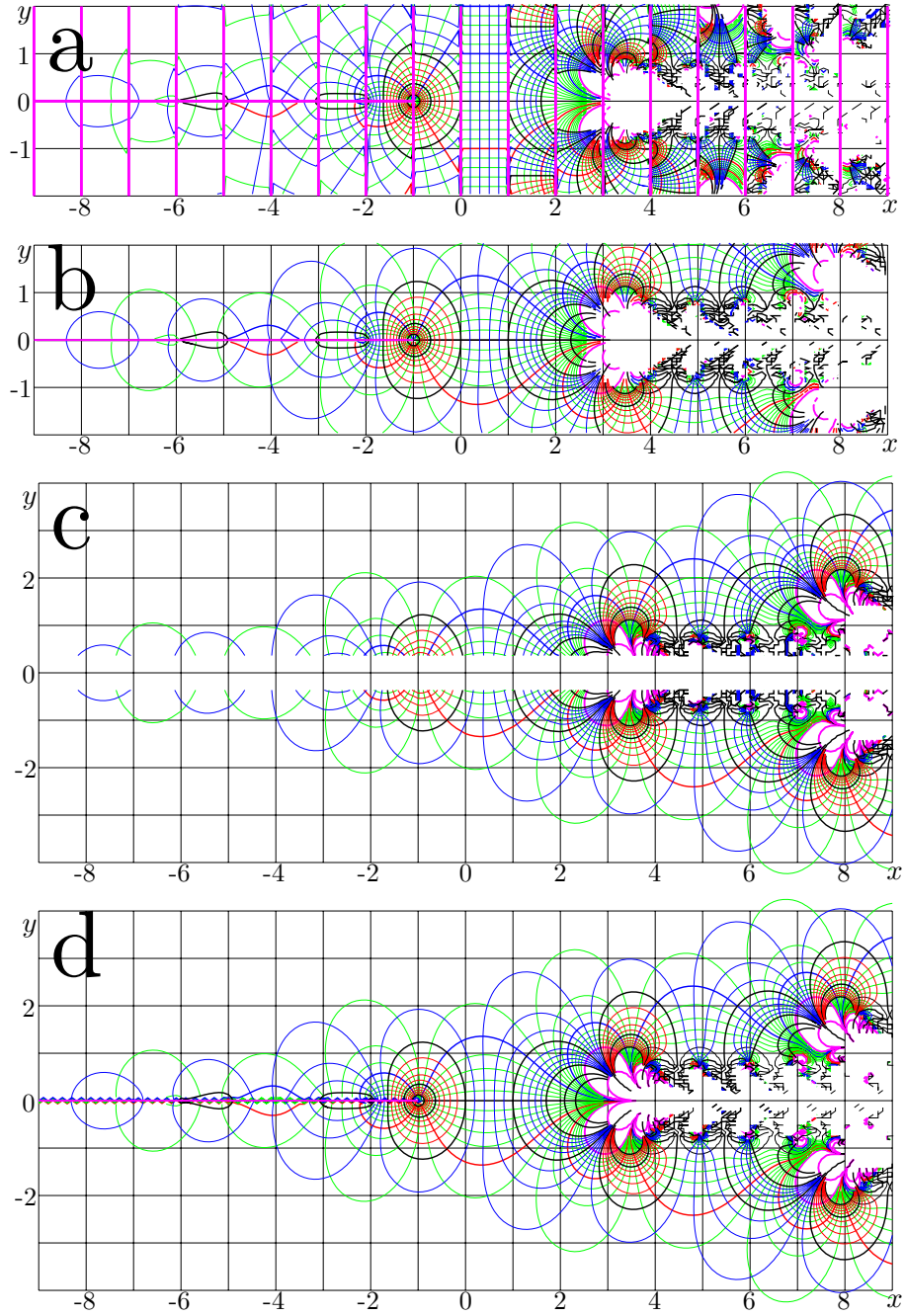


FIGURE 1. a: Function  $f = \text{uxp}(x+iy)$  by equation (1.6) at the complex plane. Levels  $|f| = 1, \exp(\pm 1), \exp(\pm 2), \exp(\pm 3), \exp(\pm 4)$  and  $\arg(f) = 0, \pm 1, \pm 2, \pm 3$  are shown with thick lines. b-d: the same for functions  $\text{Fit}_3$  by equation (1.7),  $\text{Fit}_4$  by equation (2.12), and solution  $F$  by (4.5).

the asymptotic behavior of function  $F$ , which allows to plot part (c) of the figure. I collect such guesses and assumptions in section 2.

Then, in section 3, I express the analytic tetration with the contour integral, which leads to the simple integral equation (3.6) for values of tetration at the imaginary axis.

In section 4 I describe the numerical (iterational) solution of this integral equation, which allows to evaluate function  $F$  and plot figure 1(d).

In section 5, I estimate the precision of the numerical solution, achievable with double-precision arithmetics, and provide tables of its values at the imaginary axis and those at the real axis.

In section 6, I compare the values of the analytic tetration with other solutions of equation (1.4) at the real axis.

In section 7, I suggest possible application of the formalism used to the fiber optics and generalization for other values of variables  $a$  and  $t$  in equation (1.3).

In section 8, I discuss generalization of the method for other cases of the Abel equation and complex Ackermann functions.

In section 9, I formulate the theorem about existence of analytic tetration and request for the mathematical proof.

## 2. ASSUMPTIONS

In this section I discuss some properties of the function  $\text{Fit}_3$  that are seen in figure 1 and postulate them as assumptions, as requirements for the analytic tetration  $F(z)$ .

**Assumption 0:** The analytic solution  $F$  of equation (1.4) exists, this solution is real at the real axis, and  $F(0)=1$ . (**End of Assumption 0**).

As the argument  $z$  gets out from the real axis, the approximation  $\text{Fit}_3(z)$  approaches (although it does not reach this asymptotic exactly within the range of approximation) the eigenvalues  $L$  and  $L^*$  of logarithm, which are solutions of the equation

$$(2.1) \quad L = \log(L) \quad .$$

The straightforward iteration of the equation (2.1) converges within a hundred of iterations, giving the approximation

$$(2.2) \quad L \approx 0.31813150520476413 + 1.3372357014306895 i \quad .$$

Let the analytic tetration  $F$  also approaches values  $L$  and  $L^*$  at  $\pm i\infty$  :

**Assumption 1:** Tetration  $F$  satisfies relations

$$(2.3) \quad \begin{aligned} \lim_{y \rightarrow +\infty} F(x + iy) &= L \\ \lim_{y \rightarrow -\infty} F(x + iy) &= L^* \end{aligned} \quad \text{for all real } x \quad .$$

**(end of Assumption 1)**

The imaginary part of  $\text{Fit}_3$  becomes positive at positive values of the imaginary part of the argument; this corresponds to positive values of derivative of tetration at the real axis. For initial value with positive real part and positive imaginary part, the iteration of equation (2.1) converges to  $L$ . Within the range of figure 1b, function  $\text{Fit}_3(z)$  approaches  $L$  at negative  $\Re(z)$  and positive  $\Im(z)$ , and  $\text{Fit}_3(z)$

approaches  $L^*$  at negative  $\Re(z)$  and negative  $\Im(z)$ . Let it be so for the analytic tetration  $F$  in extended range:

**Assumption 2:**

$$(2.4) \quad \begin{aligned} \lim_{x \rightarrow -\infty} F(x + iy) &= L & \text{at } y > 0 \\ \lim_{x \rightarrow -\infty} F(x + iy) &= L^* & \text{at } y < 0 \end{aligned}$$

**(end of Assumption 2)**

The iteration of logarithm leads to the exponentially convergent sequence. Hence, the function  $F(x + iy)$  at  $x \rightarrow -\infty$  should approach its limiting value exponentially. This could correspond to the following behavior:

$$(2.5) \quad F(z) = L + \exp(r + kz) + \varepsilon(z) ,$$

where  $r$  and  $k$  are complex constants,  $\Re(k) > 0$ ,  $\Im(k) > 0$ , and  $\varepsilon$  is complex function of complex variable such that

$$(2.6) \quad \lim_{x \rightarrow -\infty} \varepsilon(x + iy) = 0 \quad \text{at } y > 0 ,$$

The substitution of equation (2.5) to equation (1.4) gives the simple relation  $k = L$ . The constant

$$(2.7) \quad T = 2\pi/L \approx 1.05793999115694 - 4.44695072006701 i ,$$

is quasi-period: for moderate values of  $\Re(z)$ ,

$$(2.8) \quad F(z + T) \approx F(z) \quad \text{at } \Im(z) \gg 1$$

The conjugated symmetry should take place for the case  $\Im(z) \ll -1$ . The structure at the right upper corner of figure 1b is partially reproduced in vicinity of the central part, above the real axis; the deviations is seen only at  $y < 0.3$ . Let such behavior be property of the analytic tetration  $F$ .

**Assumption 3:**

$$(2.9) \quad \begin{aligned} F(z) &= L + \exp(Lz + r) + \varepsilon(z) & \text{at } \Im(z) > 0 \\ F(z) &= L^* + \exp(L^*z + r^*) + \varepsilon^*(z^*) & \text{at } \Im(z) < 0 \end{aligned} ,$$

where  $r$  is some fixed real number and  $\varepsilon(z)$  decays to zero faster than  $\exp(Lz + r)$  at large values of  $\Re(Lz)$  and positive  $\Im(z)$ . **(end of assumption 3).**

In order to check that this assumption is consistent with figure 1a, define functions  $F_+$  and  $F_-$  as follows:

$$(2.10) \quad F_+(z) = L + \exp(Lz + \tilde{r}) ,$$

$$(2.11) \quad F_-(z) = L^* + \exp(L^*z + \tilde{r}^*) .$$

Let

$$(2.12) \quad \text{Fit}_4(z) = \begin{cases} F_+(z) & \text{for } \Re(z) < -8, \Im(z) > 0 \\ F_-(z) & \text{for } \Re(z) < -8, \Im(z) < 0 \\ \exp(\text{Fit}_4(z-1)) & \text{for } \Re(z) \geq 8 \end{cases}$$

Function  $\text{Fit}_4$  is plotted in figure 1c for

$$(2.13) \quad \tilde{r} = 1.075 - 0.946i .$$

for  $\Im(y) > 0.3$ . In this case, in the range  $0.3 < |\Im(z)| < 2$ , function  $\text{Fit}_4(z)$  looks very similar to  $\text{Fit}_3(z)$ . I may expect that  $\tilde{r}$  approximates parameter  $r$  in equation

(2.9), although I do not use this approximate value as assumption, building up the analytic extension of tetration.

The assumptions above leave to function  $F$  almost no freedom.  $F(z)$  should have cut at  $x \leq 2$ ;  $F(n) = \text{uxp}(n)$  at integer values of  $n > -2$ ;  $F(z)$  decays at  $\pm i\infty$  to its asymptotic values according to (2.9), and it should quickly grow up in the positive direction of the real axis. In vicinity of range  $|y| < 0.2x$ , function  $F(x+iy)$  should show some complicated, quasi-periodic and perhaps fractal behavior, similar to that of  $\text{Fit}_3$  and  $\text{Fit}_4$ ; such fractal behavior is typical for iterated functions of complex variable [8].

### 3. CONTOUR INTEGRAL

In this section, the expression of the analytic tetration in terms of contour integral is suggested; this allows to replace the functional equation (1.4) for function  $F$  to the integral equation for its values at the imaginary axis.

According to the assumption of the previous section, function  $F$  is analytic. In the range of analyticity, it can be expressed with the Cauchy [13, 14, 15, 16, 17, 18] contour integral:

$$(3.1) \quad F(z) = \frac{1}{2\pi i} \oint_o \frac{F(t) dt}{t-z} \quad ,$$

where contour  $o$  evolves the point  $z$  just once.

I apply the formula Cauchy (3.1) to express tetration  $F(x+iy)$  in the range,  $|x| \leq 1$ ,  $|y| \leq A$ , where  $A$  is large positive parameter. Let the contour  $o$  consist of 4 parts:

- A. integration along the line  $\Re(t) = 1$  from  $t = -iA$  to  $t = iA$ .
- B. integration from point  $t = 1 + iA$  to  $z = -1 + iA$ , passing above point  $z$
- C. integration along the line  $\Re(t) = -1$  from  $t = iA$  to  $t = -iA$ .
- D. integration from point  $t = -1 - iA$  to  $t = 1 - iA$ , passing below point  $z$

Such a contour have several advantages. Values at the imaginary axis are related to values at the parts  $A$  and  $C$ ; as for the parts  $B$  and  $D$ , the integral can be estimated analytically, using the asymptotic values  $L$  and  $L^*$ . Then, tetration  $F$  can be expressed with four integrals:

$$(3.2) \quad F(z) = \frac{1}{2\pi} \int_{-A}^A \frac{F(1+ip) dp}{1+ip-z} - \frac{1}{2\pi} \int_{-A}^A \frac{F(-1+ip) dp}{1+ip-z} \\ - \frac{f_{\text{up}}}{2\pi i} \int_{-1+iA}^{1+iA} \frac{dt}{t-z} + \frac{f_{\text{down}}}{2\pi i} \int_{-1-iA}^{1-iA} \frac{dt}{t-z} \quad ,$$

where  $f_{\text{up}}$  is some intermediate value of function  $F$  between  $-1+iA$  and  $1+iA$ ;  $f_{\text{down}}$  is the same for points  $-1-iA$  and  $1-iA$ . Using equation (1.4), the integrands in the first two integrals can be expressed in terms of function  $F$  at the imaginary axis; the last two integrals can be simplified analytically. This gives

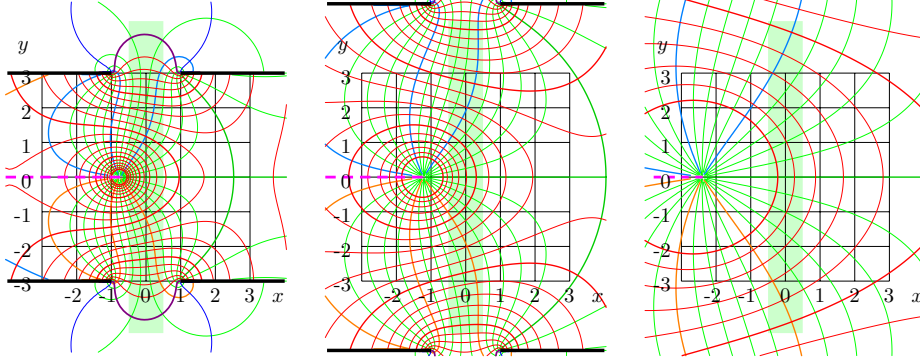


FIGURE 2. Behavior of function  $K = \mathcal{K}(x+iy)$  by (3.5) at  $A=3$  (left), 5(central) and 10(right). Levels  $|\mathcal{K}| = 1, \exp(-1), \exp(-2), \exp(-3), \exp(-4)$  and  $\arg(\mathcal{K}) = 0, \pm 1, \pm 2, \pm 3$  are shown with thick curves. Thick horizontal lines indicate the cuts of the logarithmic functions.

$$\begin{aligned}
 F(z) &= \frac{1}{2\pi} \int_{-A}^A \frac{\exp(F(ip)) dp}{1+ip-z} - \frac{1}{2\pi} \int_{-A}^A \frac{\log(F(ip)) dp}{1+ip-z} \\
 (3.3) \quad &+ f_{\text{up}} \cdot \left( \frac{1}{2} - \frac{1}{2\pi i} \ln \frac{1-iA+z}{1+iA-z} \right) + f_{\text{down}} \cdot \left( \frac{1}{2} - \frac{1}{2\pi i} \ln \frac{1-iA-z}{1+iA+z} \right)
 \end{aligned}$$

The equation (3.3) is still exact. However, it becomes approximate, when I substitute  $f_{\text{up}}$  and  $f_{\text{down}}$  to their asymptotic values, using assumptions from the previous section. Such a substitution leads to the equation for the approximation  $F_A$ :

$$(3.4) \quad F_A(z) = \frac{1}{2\pi} \int_{-A}^A \frac{\exp(F_A(ip)) dp}{1+ip-z} - \frac{1}{2\pi} \int_{-A}^A \frac{\log(F_A(ip)) dp}{1+ip-z} + \mathcal{K}_A(z),$$

where

$$(3.5) \quad \mathcal{K}(z) = L \left( \frac{1}{2} - \frac{1}{2\pi i} \ln \frac{1-iA+z}{1+iA-z} \right) + L^* \left( \frac{1}{2} - \frac{1}{2\pi i} \ln \frac{1-iA-z}{1+iA+z} \right).$$

The placement of cuts of logarithms at the transition from equation (3.2) to equations (3.3), (3.4) is not obvious; these cuts are shown in figure 2. The figure represents the map of constant modulus and constant phase of function  $\mathcal{K}$  in the right hand side of equation (3.4). This function depends on a single real parameter  $A$ ; for  $A=3$ ,  $A=5$  and  $A=10$ ; the lines  $|\mathcal{K}(z)| = \text{constant}$  and  $\arg(\mathcal{K}(z)) = \text{constant}$  are shown in the complex  $z$  plane. Thick dashed line indicates  $\arg(\mathcal{K}) = \pm\pi$ . Thick solid lines indicate the cuts of the logarithmic functions. Value of  $\mathcal{K}$  in the shaded region are required for the evaluation of tetration; then, using equation (1.4), it can be extended to the range of figure 1c and 1d. Figure 2 shows also, that just neglecting of  $\mathcal{K}$  in equation (3.4) would lead to a poor approximation; huge values of  $A$  would be necessary to obtain a good the precision.

Consider the case  $z = iy$ . This case is important, so, I give the special name to the function  $E(y) = F_A(iy)$ . At  $z = iy$ , the equation for  $E$  can be written as

follows:

$$(3.6) \quad E(y) = \frac{1}{2\pi} \int_{-A}^A \frac{\exp(E(p)) dp}{1 + ip - iy} - \frac{1}{2\pi} \int_{-A}^A \frac{\log(E(p)) dp}{1 + ip - iy} + \mathcal{K}(iy) \quad .$$

From this equation,  $E(y)$  should be found for the range  $-A \leq y \leq A$ . (The quadrature formula for the approximation may use values of the function at the tips the interval of integration.) Then, from equation (1.4), the approximation  $F_A$  of the tetration  $F(z)$  can be expressed for  $|\Re(z)| < 1$ . For the precise evaluation, value of  $z$  should be evolved by the contour, but should not approach it. For the evaluation, is sufficient to work with  $|\Re(z)| \leq 0.5$  and then extend the approximation to the whole complex plane with equation  $F$ .

The soluiton  $E$  of equation (3.6) has no need to satisfy equality  $E(0) = 1$  exactly; the correction of argument can be applied to the reconstructed tetration to satisfy condition (1.5).

In such a way, for reconstruction of the approximation  $F_A$  in the whole complex plane, it is sufficient to calculate it along the imaginary axis, or along any vertical line in the complex  $z$ -plane. The error of such approximation comes from the replacement of the function at the upper and lower contour of integration to its asymptotic values. Due to the assumption about exponential decay of the tetration  $F$  to these asymptotic values, the number of correct decimal digits at the evaluation is proportional to parameter  $A$ . Another source of error arises at the approximation of integrals as finite sums for the numerical integration. While the contour does not get too close to value  $z$ , the integration can be performed with high precision. One example of such evaluation is described in the next section.

#### 4. NUMERICAL EVALUATION OF TETRATION

For the numerical implementation, I replace the integrals in equation (3.6) with finite sums. The approximation with Laguerre-Gaussian quadrature formulas [6, 22] allow the good precision. Values  $A = 10$  and  $N = 100$  are sufficient to achieve the camera-ready quality of figures; at  $A = 24$  and  $N = 2048$ , the precise check with 14 significant decimal digits can be performed.

For the computation, values of function  $E$  are stored in a mesh with nodes at  $y_n$ , for  $n = 0..N - 1$ ; let  $E_n$  approximates  $E(y_n)$ , and let the integral of a function  $f$  be approximated as follows:

$$(4.1) \quad \int_{-A}^A f(y) dy \approx \sum_{n=0}^{N-1} W_n f(y_n)$$

Applying this rule to the equation (3.6), I get the approximation

$$(4.2) \quad E_n = \frac{1}{2\pi} \sum_{m=0}^{N-1} W_m \left( \frac{\exp(E_m)}{1 + iy_m - iy_n} - \frac{\log(E_m)}{-1 + iy_m - iy_n} \right) + \mathcal{K}(iy_n)$$

Equation (4.2) gives the straightforward way for the iterational solution; just interpret the equality as operator of assignment, updating elements of the array  $E$  one by one.

Equation (3.6) looks similar to equation of Fredholm of second kind [21, 19, 20], but the kernel is nonlinear. The soluiton is stable, at least with a good initial approximation. For the convergence, the amplitude at the center of the grid should be of order of unity; at positive values of  $y_n$  the phase should be non-negative,



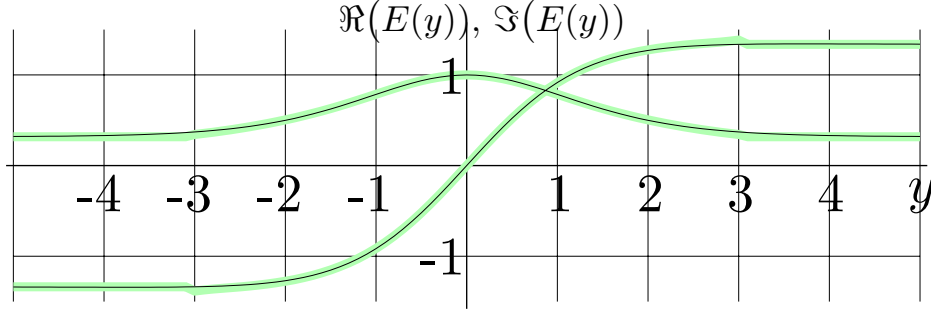


FIGURE 3. Initial condition of  $E(y)$  corresponding equation (4.3) versus  $y$  (thick lines) and the solution of equation 3.6 calculated iterating equation (4.2) (thin lines). Real and imaginary parts are plotted.

and a the negative values of  $y_n$ , the phase should be non-positive. An occasional appearance of zero in the solution gives an infinity in the evaluation of the logarithm and ruins the algorithm. In particular, the iterations do not converge with the conjugation of the function  $\text{fit}_2$  by equation (1.9) as the initial distribution. For the initial condition

$$(4.3) \quad E_n = \begin{cases} L & , \quad 3 < y_n \\ \text{Fit}_3(iy_n) & , \quad -3 \leq y_n \leq 3 \\ L^* & , \quad y_n < -3 \end{cases} ,$$

the algorithm converges to a smoothly-looking function after few updates of each point of the mesh. The typical resulting function  $E$  is in figure 3. For comparison, the initial condition is plotted with light strips. Real part of  $E$  is represented with symmetric curve, and the imaginary part corresponds to the antisymmetric curve. Visually, I would not be able to distinguish these functions from scaled and shifted  $1/\cosh$  and  $\tanh$ . At the zooming in, the defects (jumps) of the initial condition at  $|y| = 3$  are seen, while the solution (thin lines) looks perfect. After few tens iterations, the precision of the resulting solution cannot be improved more due to the rounding errors.

The discrete analogy of equation (3.4) can be written as follows:

$$(4.4) \quad F_{A,N}(z) = \frac{1}{2\pi} \sum_{n=0}^{N-1} \frac{\exp(E_n) W_n}{1 + iy_n - z} - \frac{1}{2\pi} \sum_{n=0}^{N-1} \frac{\log(E_n) W_n}{1 + iy_n - z} + \mathcal{K}_A(z) .$$

The function  $F_{A,N}$  approximates  $F$ :

$$(4.5) \quad F(z) \approx \lim_{A \rightarrow \infty} \lim_{N \rightarrow \infty} F_{A,N}(z + x_1) , \quad |\Re(z)| < 1 .$$

where  $x_1 = X_{A,N}$  is solution of equation

$$(4.6) \quad F_{A,N}(x_1) = 1 ,$$

which depends not only on  $A$  and  $N$ , but also on the initial condition, and on the mode of iterations. I use the automatic update of  $E_{N-1-n}$  each time when  $E_n$  is calculated, forcing the symmetry

$$(4.7) \quad E_{N-1-n} = E_n^* .$$

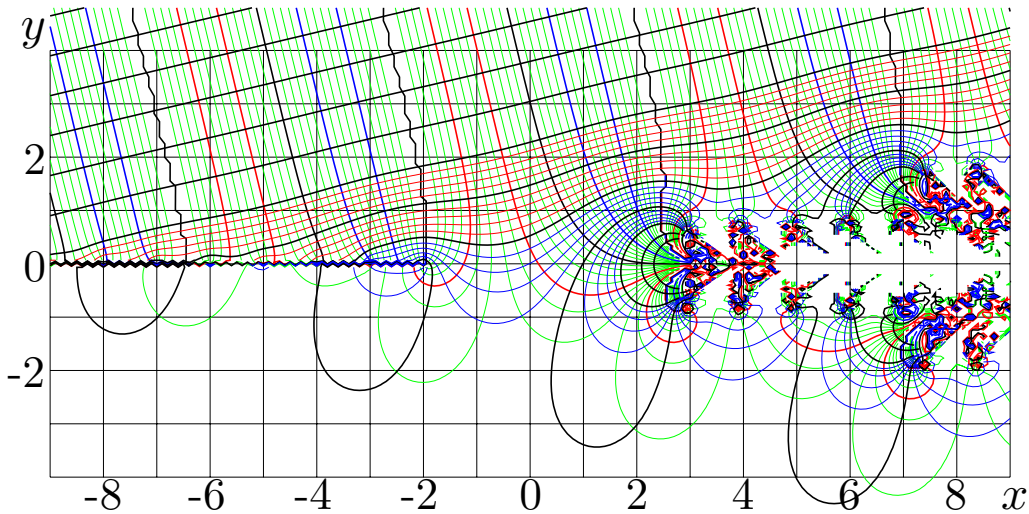


FIGURE 4. Lines of constant modulus and constant phase of  $F(x + iy) - L$  in the same notations as in figure 1. Scratched lines indicate the jumps of phase.

In this case, the displacement  $x_1$  is always real. Typically, this correction is of order of one percent. Such a displacement of the argument should be applied each time when we have constructed a function satisfying equation (1.4) and want to get a function  $F$  which satisfies also condition (1.5).

The procedure above allows to construct approximations of  $F$  within strip  $|\Re(z)| < 1$ . As the point  $z$  approaches to the contour of integration, the approximations with finite sum becomes inaccurate. Therefore, equation (4.4) should be used for reconstruction of approximations of  $F(z)$  at  $|\Re(z)| \leq 1/2$ ; values outside this range should be recovered using equation (1.4).

Function  $F$  evaluated in such a way is plotted in figure 1d. As it was mentioned, visually, it looks just as a superposition of figures 1b and 1c.

The periodic oscillations of asymptotic (2.11) is weak comparable to the quick approach of the function to the asymptotic value; this oscillation is not seen in figure 3. In order to reveal this oscillation, in figure 4, the difference  $F(z) - L$  is plotted in the same notations, as in figure 1. In the upper-left corner of the figure, the lines of constant modulus and constant phase makes almost rectangular grid, typical for the exponential function. The figure makes impression, that the small (“linear”) perturbation of the steady-state solution  $L$  of equation of tetration comes from direction  $-1.061 + 4.75 i$  and becomes strong in vicinity of real axis; The iteration of the exponential produces the quasi-periodic “garden” of self-similar “flowers” in vicinity of positive direction  $y \approx 0.22x$ . The conjugated wave of perturbation comes from the third quadrant of the complex plane. The condition (1.5) “synchronizes” these perturbations in such a way that the function  $F(z)$  becomes zero at  $z = -1$ , causing the sequence of singularities at the negative part of the real axis and cut at  $z \leq -2$ .

Table 1. Tetration  $F$  and its derivative at the imaginary axis

$y$	$F(iy)$	$F'(iy)$
$\infty$	$0.31813150520476 + 1.33723570143069 i$	$0.00000000000000 + 0.00000000000000 i$
2.2	$0.46205977590137 + 1.29516316398653 i$	$0.10524026273402 + 0.16943328263392 i$
2.1	$0.47984927595632 + 1.28360656694651 i$	$0.12642114268197 + 0.18649812732321 i$
2.0	$0.49938479980586 + 1.26976723502480 i$	$0.15095297930087 + 0.20432273436087 i$
1.9	$0.52073186937763 + 1.25329276909992 i$	$0.17918029261924 + 0.22268620786941 i$
1.8	$0.54393020954940 + 1.23379706941951 i$	$0.21142955072994 + 0.24129189880084 i$
1.7	$0.56898571838240 + 1.21086312875581 i$	$0.24798859588585 + 0.25975862529059 i$
1.6	$0.59586167470516 + 1.18404812970916 i$	$0.28908112588736 + 0.27761443401317 i$
1.5	$0.62446951205594 + 1.15289133555805 i$	$0.33483641789324 + 0.29429444323243 i$
1.4	$0.65465965324104 + 1.11692521645276 i$	$0.38525509140219 + 0.30914451353276 i$
1.3	$0.68621307873134 + 1.07569013479634 i$	$0.44017250164697 + 0.32143254761397 i$
1.2	$0.71883447558204 + 1.02875270845089 i$	$0.49922229471440 + 0.33036904052764 i$
1.1	$0.75214795374738 + 0.97572766747336 i$	$0.56180365001189 + 0.33513800375778 i$
1.0	$0.78569638858019 + 0.91630262108129 i$	$0.62705663243943 + 0.33493851305935 i$
0.9	$0.81894541361165 + 0.85026467624571 i$	$0.69385066719156 + 0.32903587645367 i$
0.8	$0.85129291145694 + 0.77752734034087 i$	$0.76079119151234 + 0.31681986197241 i$
0.7	$0.88208451053588 + 0.69815566451266 i$	$0.82624879777085 + 0.29786574159447 i$
0.6	$0.91063509163399 + 0.61238722872001 i$	$0.88841350542975 + 0.27199237376058 i$
0.5	$0.93625567282687 + 0.52064642918836 i$	$0.94537418225559 + 0.23931050362376 i$
0.4	$0.95828434050920 + 0.42354968973591 i$	$0.99521978881155 + 0.20025425056736 i$
0.3	$0.97611922542662 + 0.32189973245718 i$	$1.03615549420131 + 0.15558963085388 i$
0.2	$0.98925100004340 + 0.21666790754930 i$	$1.06662345026663 + 0.10639600379842 i$
0.1	$0.99729210719977 + 0.10896472393191 i$	$1.08541583925225 + 0.05401936304801 i$
0.0	$1.00000000000000 + 0.00000000000000 i$	$1.09176735125832 + 0.00000000000000 i$

Figures 1d and 4 confirm that the analytic tetration can be evaluated using the integral equation (3.6). Visually, the plots of the resulting approximation satisfies the requirements formulated in section 2.

## 5. ACCURACY

Plots of tetration  $F$  arise the question, how precisely can be checked its analyticity. The precision of evaluation of function  $F$  with equation (4.5) depends on parameters  $A$  and  $N$  which are supposed to be large. In this section I show, that at  $A = 24$ , using Gauss-Laguerre quadrature formula with  $N = 2048$  point and double-precision arithmetic, the residual at the substitution of approximation (4.5) to the equation (1.4) becomes of order rounding errors.

Due to the smallness of the resulting parameter  $x_1$  by equation (4.6), values of  $F(z)$  at the imaginary axis are close to values of array  $E$ . For values of  $z$ , which are integer factors of 0.1 i, approximations for  $F(z)$  are printed in Table 1. The representation (4.4) allows straightforward differentiation; so, I print the first derivative too. Similar data for the real axis are shown in table 2. At the real axis, function  $F$  is invertible; so, I print there also values of  $t = F^{-1}(x)$  which is solution of equation  $F(t) = x$ .

In order to estimate the precision of calculated values, consider the residual. From equation (1.4) it follows, that  $F(-0.5 + iy) = \ln(F(0.5 + iy))$ . At real  $y$ , both  $z = -0.5 + iy$  and  $z = 0.5 + iy$  are inside the contour  $o$  of integration and within the range of approximation, expected for the function  $F_{A,N}(z)$ . Functions  $F_{A,N}(-0.5 + iy)$  and  $F_{A,N}(0.5 + iy)$  are shown in the top part of figure 5. The

Table 2. Tetration  $F$ , its derivative, and its inverse at the real axis

$x$	$F_{A,N}(x + x_1)$	$F(x)$	$F'(x)$	$F^{-1}(x)$
-1.1	-0.00000001547015	-0.11279679776258	1.16819644635938	-1.67261575378528
-1.0	-0.00000000000000	-0.00000000000000	1.09176735125833	-1.63635835428603
-0.9	0.10626039927151	0.10626040042411	1.03653178245952	-1.59610183735171
-0.8	0.20785846728047	0.20785846728047	0.99791089741917	-1.55146594044381
-0.7	0.30629553437625	0.30629553437625	0.97291281085669	-1.50206743429127
-0.6	0.40282959178360	0.40282959178360	0.95959569174883	-1.44753575532149
-0.5	0.49856328794111	0.49856328794111	0.95675517789104	-1.38753447917073
-0.4	0.59450765927989	0.59450765927989	0.96374036331481	-1.32178907507892
-0.3	0.69163169510089	0.69163169510089	0.98034861830628	-1.25012048301963
-0.2	0.79090416202613	0.79090416202613	1.00677283707697	-1.17248262296575
-0.1	0.89333216876936	0.89333216876936	1.04358746497488	-1.08900005343708
0.0	1.00000000000000	1.00000000000000	1.09176735125832	-1.00000000000000
0.1	1.11211143309340	1.11211143309340	1.15273884603792	-0.90603157029014
0.2	1.23103892493161	1.23103892493161	1.22846715833643	-0.80786507256596
0.3	1.35838369631113	1.35838369631113	1.32158890019997	-0.70646669396340
0.4	1.49605193039935	1.49605193039935	1.43560498704373	-0.60294836953664
0.5	1.64635423375119	1.64635423375119	1.57515793778431	-0.49849837513117
0.6	1.81213853570187	1.81213853570186	1.74643105077407	-0.39430303318768
0.7	1.99697132461831	1.99697132461829	1.95772807888681	-0.29147201034755
0.8	2.20538955455274	2.20538955455274	2.22032629869699	-0.19097820800866
0.9	2.44325711324446	2.44325744833852	2.54975284679259	-0.09361896280296
1.0	0.59665094765656	2.71828182845904	2.96773135183036	0.00000000000000
1.1	0.00000003298313	3.04077200774189	3.50521601526880	0.08946084201600

bottom part of figure 5 shows the real and imaginary parts of

$$(5.1) \quad \text{residual}(y) = F_{A,N}(-0.5 + iy) - \ln(F_{A,N}(0.5 + iy)) \quad .$$

For  $A = 24$  and  $N \geq 1024$ , at the double-precision arithmetic, the typical values of this residual are of order of  $10^{-14}$ . The residual characterizes the error of evaluation of function  $F$ , then the error of values in tables 1,2 is expected to be of order of unity in the last decimal digit of the mantissas.

The smooth trends in lower part of Figure 5 are symmetric for the real part and anti-symmetric for the imaginary part; these trends should be attributed to the finiteness of the parameter  $A$ . (for smaller values  $A = 20$ , this trends were two orders of magnitude larger, and the deviation was at the level  $10^{-12}$ .) The irregular structure in figure 5 appears due to the rounding errors. For double-precision arithmetics, value  $A = 24$  provides a reasonable compromise between the speed of evaluation and the precision: the error due to replacement  $f_{\text{up}}$  and  $f_{\text{down}}$  to the asymptotic values  $L$  and  $L^*$  and rounding errors give comparable contributions to the error of the resulting approximation.

Similar relation can be checked at the real axis; while the real part of the argument of the function  $F_{A,N}$  does not exceed 0.8, the relation

$$(5.2) \quad F_{A,N}(x - .5) - \log(F_{A,N}(x + .5)) \approx 0$$

holds with 14 decimal digits. The left part of this equation scaled up with factor  $10^{13}$  is plotted at the bottom of figure 6. The same data are used in Table 2. The zeroth column has sense of the argument  $x$ ; in this table, this argument runs real values from  $-1.1$  to  $1.1$ . It is the same  $x$  that appears in the figure 6.

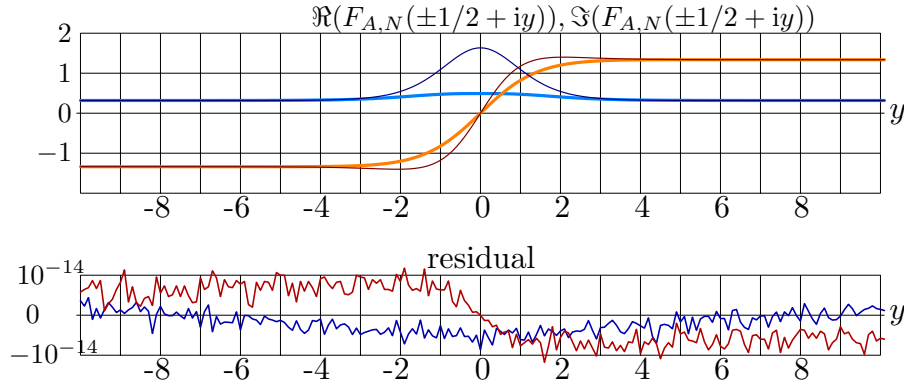


FIGURE 5. Real and imaginary parts of  $F(\pm 1/2 + iy)$  reconstructed at the array of  $N = 2048$  nodes; function  $F$  reconstructed along the lines  $z = 0.5 + iy$  and  $z = -0.5 + iy$ , top; residual  $F(-0.5 + iy) - \log(F(0.5 - iy))$ , real and imaginary parts, bottom.

The first column represents the corresponding estimate  $F_{A,N}(x + x_1)$ , evaluated with equation (4.5) using value  $x_1 = -0.00743143611046$ . This value is specific for  $A = 24$ ,  $N = 2048$ , initial condition (I used approximation  $\text{Fit}_3$  in the central part of the initial distribution), on the order of updating values at the iterational solution, and even on maximal number of iterations, because the value at the center is not fixed; it drifts from iteration to iteration, decreasing for  $\sim 10^{-13}$  per cycle of iterations. Indeed, 64 iterations were sufficient to make errors of the approximation comparable to the rounding errors at the double-precision arithmetic.

However, the third column approximates the tetration  $F$  only in the central part of the table; at values  $|x| > 0.8$ , the point  $x$  is too close to the contour of integration. Therefore, I offer the second column, where, at  $|x| > 0.5$ , the value of tetration is estimated with equation (1.4); in the central part it coincides with the first column. This central part has length larger than unity, which confirms the high precision of the evaluation.

The third column is derivative of tetration  $F$ . For the extension of the approximation to values  $|x| > 0.5$ , the following relations were used:

$$(5.3) \quad F'(z + 1) = F'(z) \exp(F(z)) , \quad F'(z - 1) = F'(z)/F(z) ,$$

The fourth column shows the inverse function; for each  $x$ , it contains value  $t$  such that  $F(t) \approx x$ ;  $|F(t) - x|$  is estimated to be of order of  $10^{-14}$ .

In such a way, the first column of the table serves as confirmation of the procedure, while the last two shows the behavior of tetration at the real axis.

I used the Laquerre-Gaussian quadrature with  $N = 2048$  nodes in order to get wide region with good approximation,  $|x| < 0.8$ , and to confirm that the equation  $F(x + 1) = \exp(F(x))$  holds with many decimal digits. At the evaluation of the function in the range  $|x| \leq 0.5$ , the same precision can be obtained with  $N \sim 1024$ . The moderate number of nodes of the mesh is sufficient for the precise evaluation of the function  $F$ ; this indicates the stability of the algorithm.

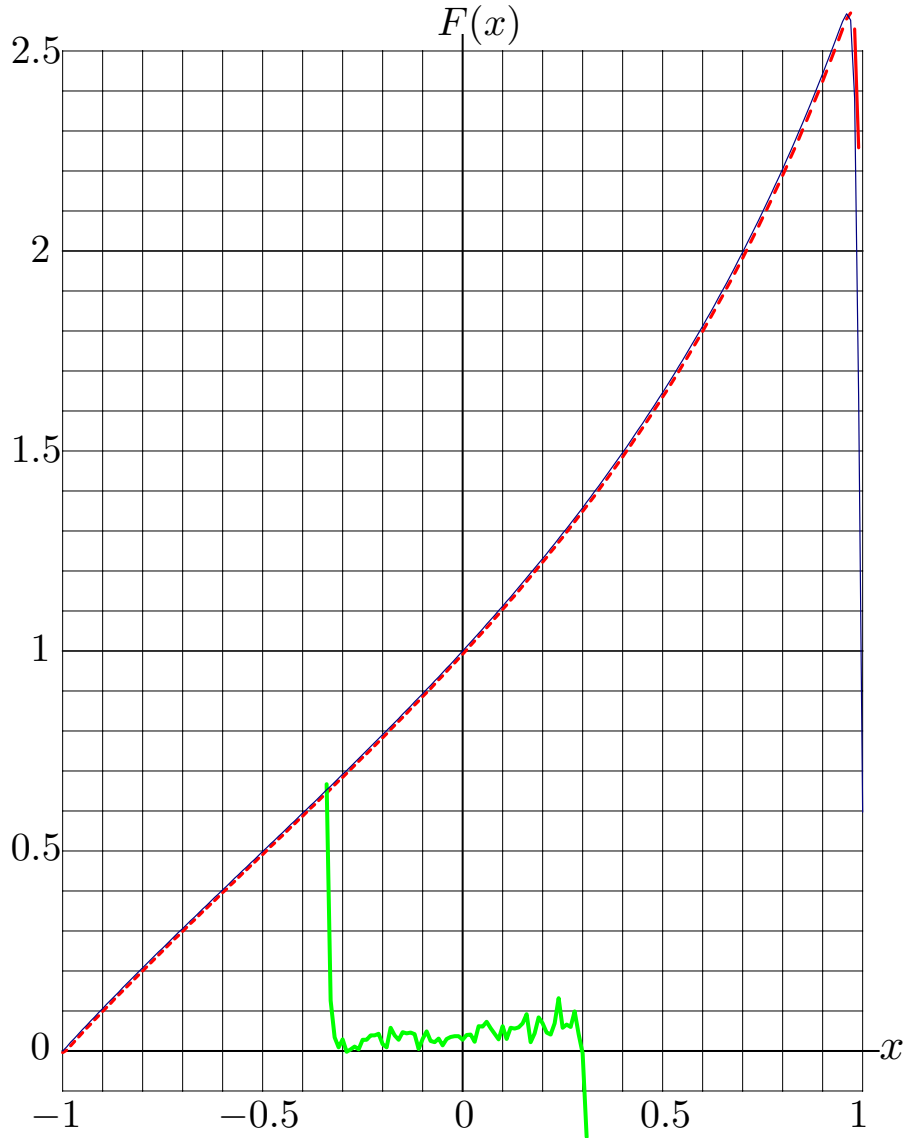


FIGURE 6. Bottom: left hand side of equation (5.2) scaled with factor  $10^{13}$ . Central part: approximation  $F_{A,N}(x)$  by equation (5.2) (dashed) and its correction  $F_{A,N}(x+x_1)$  (solid).

For the fast convergence,  $A$  should be of order of twiced number of correct decimal digits required in the estimate, and the initial condition for the array  $E$  should have values of order of  $L$  at  $y \gg 1$  and of order of  $L^*$  at  $y \ll 1$ . In particular, fast convergence takes place when the fit  $\text{Fit}_3$  is used for central part of the initial distribution.

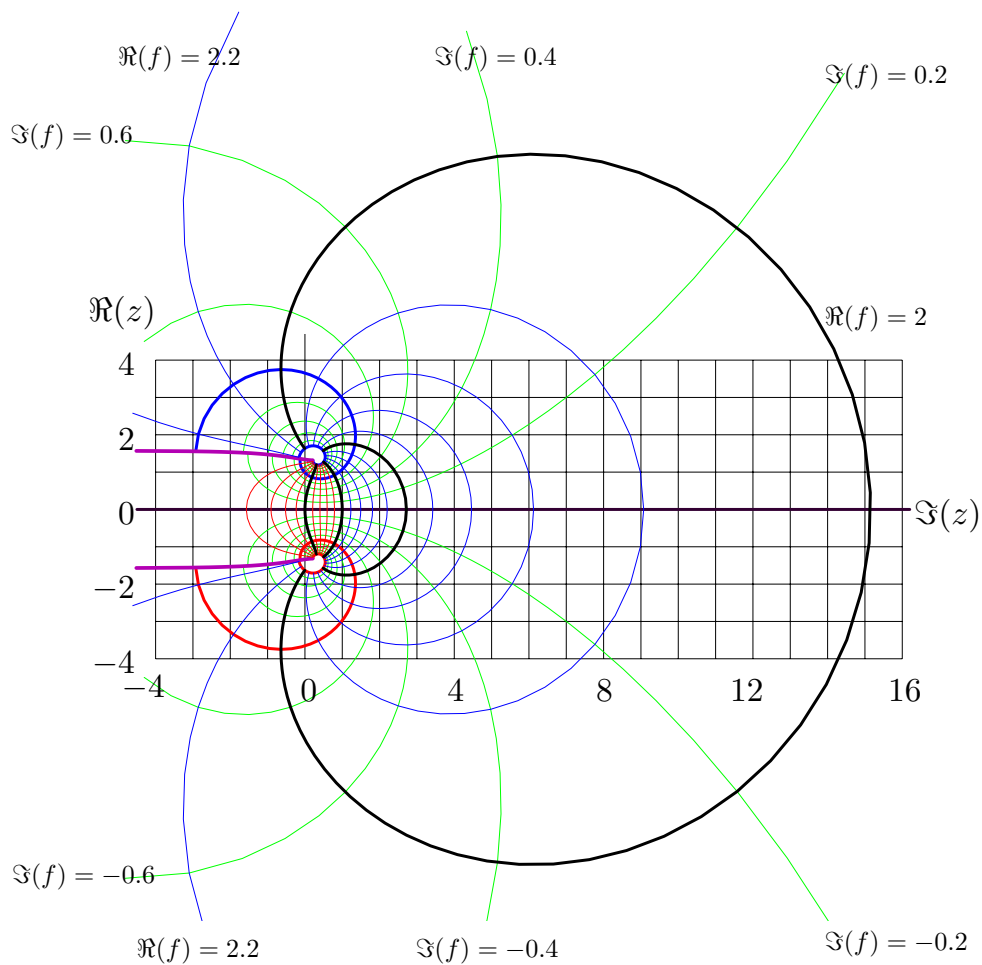


FIGURE 7. Function  $f = F^{-1}(z)$  by equation (6.1) in complex  $z$ -plane. Levels  $\Re(f) = -2, -1, 0, 1, 2$  and  $\Im(f) = -2, -1, 0, 1, 2$  (thick lines) and intermediate levels (thin lines).

## 6. INVERSE FUNCTION

Consider the inverse function  $F^{-1}$  such that

$$(6.1) \quad F(F^{-1}(z)) = z .$$

This function is shown in Figure 7. Function  $F^{-1}$  has singularities at eigenvalues  $L$ ,  $L^*$  of logarithm. These singularities are bifurcation points. In order to simplify the comparison with Table 2, it is convenient to put the cuts along levels  $\Re(F^{-1}(z)) = -2$ . In this case, function  $F^{-1}$  has no singularities at the real axis. As  $\Re(z) \rightarrow -\infty$ , function  $F^{-1}(z)$  approaches its asymptotic value  $-2$  in the whole strip between cuts. In the positive direction of real axis, function  $F^{-1}$  grows slowly (slower than any logarithm), which corresponds to the rapid growth of tetration  $F$ .

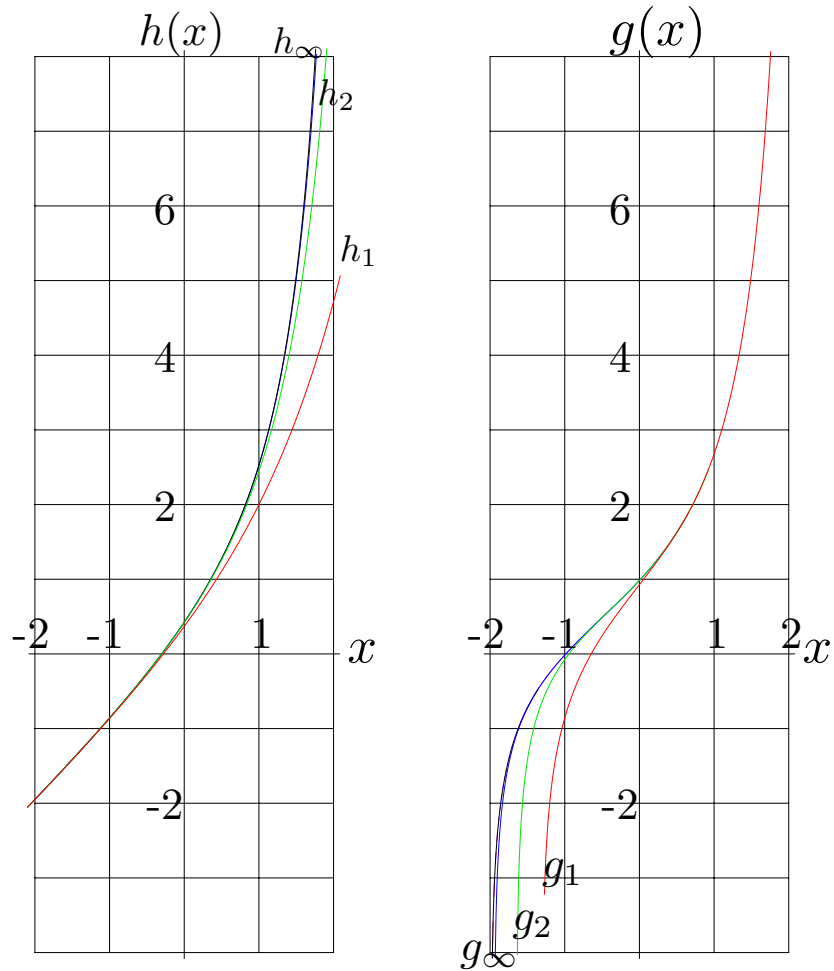


FIGURE 8. Functions  $h_1, h_2, h_\infty$  by equations (7.1),(7.2);  $g_1, g_2, g_\infty$  by equations (7.3),(7.4). In the graphics,  $h_3$  almost overlaps with  $h_\infty$  and  $g_3$  almost coincides with  $g_\infty$ , although the differences can be seen at the zooming in.

## 7. OTHER TETRATIONS

The results above refer to the specific function that becomes eigenvalue of logarithm (2.2) at  $\pm i\infty$ . However, different requirements may lead to different tetrations. I compare them in this section. I could not yet construct another analytic tetrations in the complex plane. Therefore this section refers to the tetration at the real axis.

We may require, that the tetration is defined as a sequence of differentiable functions. An example of such a sequence is constructed below. Let

$$(7.1) \quad \begin{aligned} h_0(x) &= x, \\ h_n(x) &= x + \exp(h_{n-1}(x-1)) \quad \text{for integer } n > 0. \end{aligned}$$



Table 3. Comparison of various tetrations

$x$	$\text{uxp}(x)$	$g_\infty(x-x_0)$	$\text{Fit}_3(x)$	$F(x)$
-1.1	-0.105360515658	-0.112273219465	-0.112743778423	-0.112796797763
-1.0	0.000000000000	-0.000000000001	0.000000000000	-0.000000000000
-0.9	0.100000000000	0.106179688230	0.106412412786	0.106260400424
-0.8	0.200000000000	0.208093402820	0.208104295564	0.207858467280
-0.7	0.300000000000	0.307095312397	0.306588453868	0.306295534376
-0.6	0.400000000000	0.404237363416	0.403131965155	0.402829591784
-0.5	0.500000000000	0.500408437490	0.498845079828	0.498563287941
-0.4	0.600000000000	0.596458714817	0.594745797295	0.594507659280
-0.3	0.700000000000	0.693307316434	0.691810291661	0.691631695101
-0.2	0.800000000000	0.792014962172	0.791015663894	0.790904162026
-0.1	0.900000000000	0.893800020573	0.893379533907	0.893332168769
0.0	1.000000000000	0.999999999999	1.000000000000	1.000000000000
0.1	1.105170918076	1.112021675762	1.112280500628	1.112111433093
0.2	1.221402758160	1.231328173701	1.231341586317	1.231038924932
0.3	1.349858807576	1.359470536292	1.358781651654	1.358383696311
0.4	1.491824697641	1.498159513017	1.496504365065	1.496051930399
0.5	1.648721270700	1.649394807818	1.646818228388	1.646354233751
0.6	1.822118800391	1.815677569929	1.812570126163	1.812138535702
0.7	2.013752707470	2.000320297393	1.997328008677	1.996971324618
0.8	2.225540928492	2.207840662685	2.205635473317	2.205389554553
0.9	2.459603111157	2.444400798181	2.443373176304	2.443257448339
1.0	2.718281828459	2.718281828457	2.718281828459	2.718281828459
1.1	3.019740552946	3.040499088409	3.041286147031	3.040772007742

First elements of this sequence are plotted in left hand side of figure 8. The terms with  $h$  of negative arguments give exponentially small contribution; so, this sequence converges rapidly. Consider the limit

$$(7.2) \quad h_\infty(x) = \lim_{n \rightarrow \infty} h_n(x) .$$

Function  $h$  has rapid growth, similar to that of tetration. Their logarithms behave even more similarly. So, consider the functional sequence  $g$  such that

$$(7.3) \quad \begin{aligned} g_0(x) &= h_\infty(x) , \\ g_n(x) &= \log(g_{n-1}(x+1)) \text{ for integer } n > 0 . \end{aligned}$$

For  $x > -2$ , this sequence also converges; the first few elements are shown in the right hand side of the figure 8. The limit

$$(7.4) \quad g_\infty(x) = \lim_{n \rightarrow \infty} g_n(x) .$$

satisfies the first of equations (1.4); the second equation can be satisfied if I define

$$(7.5) \quad F_g(x) = g_\infty(x-x_0) ,$$

where  $x_0$  is solution of equation

$$(7.6) \quad g_\infty(x_0) = 1 .$$

This equation can be solved numerically, giving value  $x_0 \approx 0.014322263393$  . I compare such a tetration with function  $F$  in Table 3.

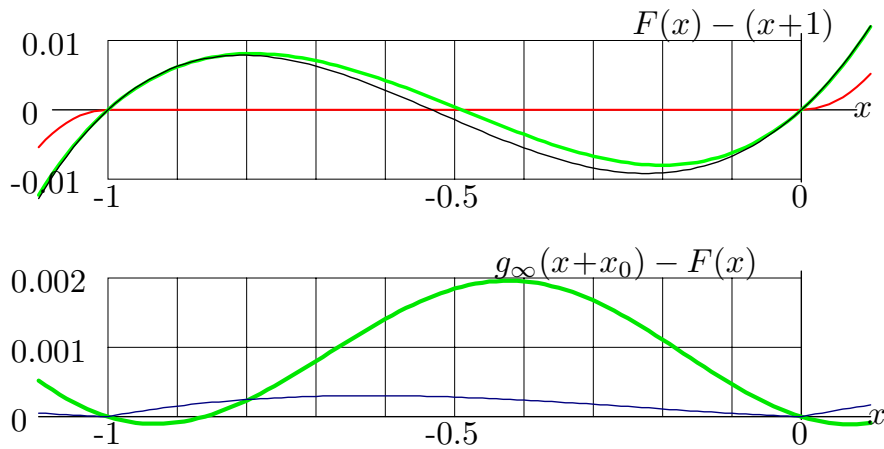


FIGURE 9. Comparison of various tetrations for real argument. Upper graphic: Tetrations with subtracted linear part:  $\text{uxp}(x) - (x+1)$  (lies at the abscissa axis),  $g_\infty(x+x_0) - (x+1)$  (thick curve), and  $F(x) - (x+1)$  (thin curve). Lower graph: differences  $g_\infty(x+x_0) - F(x)$  (thick line) and  $\text{Fit}_3(x) - F(x)$  (thin line).

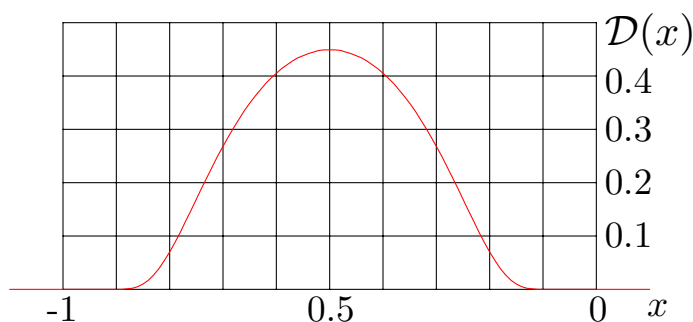
At the real axis, in the range from minus unity to zero, every tetration  $F(x)$  look similar to the function  $1+x$ . In figure 9, I plot the difference between tetrations and this linear function. All the tetrations happen within a strip of width equal to 1%; the  $\text{uxp}$  function by (1.6) in this range just coincides with the abscissa axis, and all the tetrations deviate for less than one percent from  $\text{uxp}$ . Function  $g_\infty(x-x_0) - (1+x)$  is shown with thick line, and function  $F(x) - (1+x)$  is plotted with thin line. The difference  $g_\infty(x-x_0) - F(x)$  is plotted in the lower part of figure 9. At the same graphic, I plot also  $\text{Fit}_3(x) - F(x)$ . In the range  $-1 \leq x \leq 0$ , the error of the approximation  $\text{Fit}_3$  is of order of  $10^{-4}$ .

The sinusoidal-like difference  $g_\infty(x-x_0) - F(x)$  may mean, that there exist some analytic extension of  $g_\infty$ , growing exponentially in the direction of imaginary axis with increment of order of  $2\pi$ . The construction of such alternative analytic tetration may be matter for the future research.

## 8. FIBER OPTICS AND THE ABEL EQUATION

Pure mathematicians should skip this section; there are only speculations and no new formulas here. In this section I discuss the possible application of the algorithm used to calculate  $F$  above to the recovery of an analytic function from the recurrent equation.

Assume that one Manufacturer offers to some Scientist one piece of fiber of length, say, one meter, in exchange that the Scientist investigates and reports its nonlinear properties; but Manufacturer does not allow the Scientist to cut the fiber to smallest pieces. In the following I treat this fiber as a single-dimensional homogeneous object. To be more specific, let the fiber to be optical amplifier, with some transfer function  $H$ . I assume that the signal in the fiber is determined by its intensity. (This assumption trashes out many physical effects.) The laboratory of

FIGURE 10. Graphic of function  $\mathcal{D}$  by equation (8.2).

Scientist is assumed to be well equipped, so, the Scientist can launch the signal of calibrated power and measure the transfer function  $H$  with so many decimal digits as he needs. Assume, he counts also with with an advances software, which allows him to invert the transfer function and to extend it to the complex plane. In other words, Scientist knows everything about the transfer function  $H$ , but Scientist is not allowed is to open the jacket of the fiber and to measure the power inside; he just believes Manufacturer that the fiber is uniformly pumped. The signal power as function of length of propagation is supposed to be continuous and analytic. How to reconstruct this function in a long fiber, assuming, that at the coordinate zero, the signal power is just one Watt?

Such a problem leads to the Abel equation [10, 11]

$$(8.1) \quad \varphi(z+1) = H(\varphi(z)) \quad ;$$

$\varphi(x)$  may have sense of logarithm of power of the signal in the fiber at coordinate  $x$ . In the case of  $H = \exp$ , this equation becomes (1.4), and  $F$  is one of its solutions. The Scientist knows the value of function  $F$  at integer points, and wants to reconstruct the behavior in the whole real axis. In the similar way, if the Scientist has no idea about Gamma-function, he could “reconstruct” values of factorial at the non-integer values of its argument using transfer function  $H(z, f) = zf$ ; in this case, the transfer function has an additional argument, but it still leads to the recursive equation.

The simple approach could be just linear approximation. Choose one segment of unit length, approximate the solution with linear function at this segment and extend this approximation to the whole range, using equation 8.1. Such an approach is an analogy to the definition of ultraexponential  $\text{uxp}(x)$  by [3] at the segment  $-1 \leq x \leq 0$  and the extension to the real axis using the equation 1.4.

However, the Scientist may also expect, that function  $F$  is analytic, and reconstruct the solution of equation (8.1) with desired behavior at  $\pm i\infty$ , just replacing  $\exp$  and  $\log$  in the equations (3.3), (3.6), (4.2), (4.4) to  $H$  and  $H^{-1}$ .

The requirement of analyticity of the reconstructed function is much stronger that just existence of all the derivatives along the real axis. Leaving from the real axis is important not only for efficiency of the evaluating algorithms, but also for the uniqueness of the solution. At the real axis, various differentiable functions may satisfy the equation (1.4), even if the additional requirement of the existence of all derivatives is applied. Let  $F$  be the solution; consider the new function

$G(x) = F(x) + \alpha \mathcal{D}(x)$  defined at the range  $0 \leq x \leq 1$  and extended to the positive values of  $x$  using (1.4). Let  $\alpha = \text{constant}$  and  $\mathcal{D}(x)$  is function differentiable along the real axis (at least,  $-1 \leq x \leq 0$ ), which vanishes with all its derivatives at  $x = -1$  and  $x = 0$ . Such a function can be

$$(8.2) \quad \mathcal{D}(x) = \begin{cases} \exp(-0.1/x^2 - 0.1/(x+1)^2) & , \quad (x+1)x \neq 0 \\ 0 & , \quad (x+1)x = 0 \end{cases} .$$

The graphic of this function is shown in figure 10. At the real axis, function  $\mathcal{D}(x)$  has all the derivatives; in particular, in points  $x = -1$  and  $x = 0$ ; and all these derivatives are zero in these points. Then, the function  $G$  is also solution, and has all its derivatives along the real axis.

The difficulties with reconstruction of real-differentiable and real-analytic functions seem to be typical for the analytic extension of a function to the real axis [1], and the extension to the complex plane seems to be essential for the robust evaluation at non-integer values of the argument.

## 9. DISCUSSION

The precise numerical evaluation of analytic tetration, that remains limited at the imaginary axis, aimed to catch any contradiction, following from the assumption of its existence. Such a contradiction could provide a hint to the generalization of the proof of the non-existence by [3]. No such contradictions were detected. Perhaps, the analytic extensions or tetration exist, and one of them remains limited at  $\pm i\infty$ . The construction of solutions growing up at  $z \rightarrow \pm i\infty$  and their identification with solutions constructed for real axis  $z > -2$  [1, 12] can be continuation of this work.

The method of recovery of an analytic function with required behavior at  $\pm i\infty$  may be useful also for more general equation (8.1). In particular, at  $H(f) = \exp_a(f)$ , the equation becomes

$$(9.1) \quad F(x+1) = \exp(\ell F(x)) ;$$

where  $\ell = \ln(a)$ . At real values of  $\ell$  of order of unity, this equation can be treated with similar contour integrals. At  $\ell = \ln(2)$  such an extension applies to the fourth Askermann function  $A_4$ , using relation 1.1. Such a generalization may be continuation of this work. The method may be useful in various applications and in particular in nonlinear fiber optics, while the behavior of some parameter along the fiber can be recovered from the transfer function of a piece of fiber. The practical application of such a recovery may be matter for the future research.

The function  $F^{-1}$ , approximated in the table 2 for the real axis is only a special example. In general, the recursive exponential  $\exp_a^z(t)$  may be treated as function of 3 variables; then it may have 3 different kinds of inverse functions. The analysis of the analytic properties of such functions and the precise evaluation may be matter for the future research.

Similar approach can be used for the evaluation of elements of the functional sequence, determined with equations

$$(9.2) \quad F_3(z) = \exp(z) ,$$

$$(9.3) \quad F_n(z+1) = F_{n-1}(F_n(z)) \text{ for integer } n ,$$

$$(9.4) \quad F_n(0) = 1 \text{ for integer } n \geq 3 ,$$

and condition that these functions remain analytic and finite at  $i\infty$ . Such a sequence may be a complex analogy of the Ackermann functions [2]. Then, tetration  $F$ , considered above, appears as  $F_4$ ; pentation appears as  $F_5$ , and so on. Tetration  $F_4$  is already required for mathematics of computation, although it is not yet implemented as an upgrade of the floating point; pentation  $F_5$  and highest operations in this hierarchy may be requested in future.

## 10. CONCLUSION

The numerical solution of equation (1.4) is consistent with requirements (1.5), (2.3) and (2.4) within 14 decimal digits. Such agreement hints to the following theorem.

**Theorem 0.** There exist solution  $F(z)$  of equation (1.4), analytic in the whole complex  $z$ -plane except  $z \leq 2$  and real at  $z > 2$ , such that  $F(1) = 0$ , and, at  $\Im(z) > 0$ ,

$$(10.1) \quad F(z) = L + \mathcal{O}(e^{Lz}) ,$$

where  $L \approx 0.31813150520476413 + 1.3372357014306895 i$  is eigenvalue of logarithm ( $L = \ln(L)$ ). There exist only one such solution of equation (1.4). (**end of Theorem**).

The proof of such a theorem may be matter for the future research. The method of recovery of an analytic function with required properties at  $\pm i\infty$  from the transfer function may work also for more general equation (8.1). The application for the analytic extension of  $\exp_a^z(t)$  of different bases (in particular  $a=2$ ) is straightforward. The same method may be used in physics and, in particular, in fiber optics.

## ACKNOWLEDGEMENT

Author is grateful to K.Ueda and J.-F.Bisson for the stimulating discussions. This work was supported by the 21st Century COE program of the Ministry of Education, Science and Culture of Japan.

## REFERENCES

1. P.Walker. Infinitely differentiable generalized logarithmic and exponential functions. Mathematics of computation, **196** (1991), 723-733.
2. W.Ackermann. "Zum Hilbertschen Aufbau der reellen Zahlen". Mathematische Annalen **99**(1928), 118-133.
3. M.H.Hooshmand. "Ultra power and ultra exponential functions". Integral Transforms and Special Functions **17** (8), 549-558 (2006)
4. N.Bromer. Superexponentiation. Mathematics Magazine, **60** No. 3 (1987), 169-174
5. R.L.Goodstein. Transfinite Ordinals in Recursive Number Theory. J.of Symbolic Logic, **12**, (1947), p.123-129
6. M.Abramovitz, I.Stegun. Table of special functions. National Bureau of Standards, New York, 1970.
7. I.S.Gradshstein, I.M.Ryshik, 1980. Tables of Integrals, Series and Products. Academic, New York.
8. I.N.Baker, P.J.Rippon,"A Note on Complex Iteration." Amer.Math.Monthly **92** (1985), 501-504.
9. J.F.MacDonnell, Some critical points of the hyperpower function  $x^{x^{\dots^x}}$  International Journal of Mathematical Education, 1989, V.20, #2, p.297.
10. J.Laitochova. Group iteration for Abels functional equation. Nonlinear Analysis: Hybrid Systems **1**(2007), 95-102.

11. G.Belitskii, Yu.Lubish "The real-analytic solutions of the Abel functional equations". *Studia Mathematica* **134**(1999), 135-141.
12. D.Kouznetsov. Analytic generalization of tetration. *Japanese Journal of Mathematics*, 2008, under consideration. Preprint: [www.ils.uec.ac.jp/~dima/PAPERS/uxp.pdf](http://www.ils.uec.ac.jp/~dima/PAPERS/uxp.pdf)
13. G.Arften, "Cauchy's Integral Formula." 6.4 in *Mathematical Methods for Physicists*, 3rd ed. Orlando, FL: Academic Press, pp. 371-376, 1985.
14. W.Kaplan, "Cauchy's Integral Formula." 9.9 in *Advanced Calculus*, 4th ed. Reading, MA: Addison-Wesley, pp. 598-599, 1991.
15. K.Knopp, "Cauchy's Integral Formulas." Ch. 5 in *Theory of Functions Parts I and II, Two Volumes Bound as One, Part I*. New York: Dover, pp. 61-66, 1996.
16. S.G.Krantz, "The Cauchy Integral Theorem and Formula." 2.3 in *Handbook of Complex Variables*. Boston, MA: Birkhuser, pp. 26-29, 1999.
17. Morse,P.M. and Feshbach,H. *Methods of Theoretical Physics, Part I*. New York: McGraw-Hill, (1953),p. 367-372.
18. F.S.Woods, "Cauchy's Theorem." 146 in *Advanced Calculus: A Course Arranged with Special Reference to the Needs of Students of Applied Mathematics*. Boston, MA: Ginn, pp. 352-353, 1926.
19. K.Atkinson. An Automatic Program for Linear Fredholm Integral Equations of the Second Kind. *ACM Transactions on Mathematical Software* **2**(1976), 1403-1413,
20. N.K.Albov. On a criterion for solvability of Fredholm equations. *Math. USSR Sb.* **55**(1986), 113-119.
21. J.Guy, B.Mangeot and A. Sales. Solutions for Fredholm equations through nonlinear iterative processes. *J.Phys.A* **17**(1983), 1403-1413.
22. W.H.Press, S.A.Teukolsky, W.T.Vetterling. B.P.Flannery. *Numerical Recipes in C*. Cambridge University Press, 1992

*Current address:* Institute for Laser Science, University of Electro-Communications 1-5-1 Chofu-Gaoka, Chofu, Tokyo, 182-8585, Japan

*E-mail address:* [dima@ils.uec.ac.jp](mailto:dima@ils.uec.ac.jp)